Quantum study of the redistribution of flux during inelastic collisions

Millard H. Alexander

Citation: The Journal of Chemical Physics **95**, 8931 (1991); doi: 10.1063/1.461225
View online: http://dx.doi.org/10.1063/1.461225
View Table of Contents: http://scitation.aip.org/content/aip/journal/jcp/95/12?ver=pdfcov
Published by the AIP Publishing

Quantum study of the redistribution of flux during inelastic collisions

Millard H. Alexander
Department of Chemistry and Biochemistry, University of Maryland, College Park, Maryland 20742

(Received 7 August 1991; accepted 9 September 1991)

A new method is presented for the study of the mechanism of inelastic atomic and molecular collisions. This involves the determination of the current density associated with, separately, the incoming and outgoing scattering wave functions in either an asymptotic (diabatic) or locally adiabatic basis. This yields a picture of how the incoming flux, initially associated with a given internal state, redistributes itself as a function of the interparticle separation both as the particles approach, and, subsequently, as the particles recede. It is shown that the separation into incoming and outgoing flux, which is valid asymptotically, continues to be valid as the collision partners approach, without mixing of the contributions from the incoming and outgoing waves. A simple extension of our linear-reference-potential, log-derivative propagation technique can be used to compute the redistribution of the initial flux. It is argued that analysis in a fully adiabatic basis, which corresponds to the local eigenvectors of the collision system, provides the most meaningful physical insight. A simple stabilization correction can be introduced, which prevents adiabatically closed channels from numerically contaminating the determination of flux redistribution among the locally open channels. Application is made to a pedagogical two-state problem, to a multistate collision system involving four different electronic potential curves, and to a second multistate collision system involving a closed-channel resonance.

I. INTRODUCTION

In the quantum description of inelastic collisions between particles with internal degrees of freedom, the standard technique for the solution of the underlying multidimensional, time-independent Schrödinger equation involves expansion in a complete set of states in the internal degrees of freedom. The expansion coefficients, which depend implicitly on the separation between the two particles, are themselves solutions to a set of ordinary differential equations, the "close-coupled" (CC) equations.[1-3] By matching the asymptotic form of these solutions to the known collisional or photodissociation boundary conditions, one obtains the S matrix, which contains all the dynamically relevant information. One criticism of this method is that information on the transfer of flux from a particular initial state to a given final state is readily accessible only asymptotically, at large interparticle separations, after the collision is finished. Thus little "mechanistic" insight is obtained.

Such information is readily obtained from time-dependent methods, either those based on a classical treatment of the interparticle motion,[4-7] or those based on a fully quantum, time-independent, solution of the Schrödinger equation.[8] Kouri and co-workers have recently presented a time-dependent, wave-packet-based treatment of inelastic collisions within the conventional coupled-channel development.[9-13] A good example of the use of this close-coupled wave-packet (CC-WP) method to examine inelastic energy transfer during a collision is seen in the recent work of Corey and Lemoine on collisions of NO with a silver surface.[14,15]

In the present article we report the development of an analogous technique within the time-independent close-coupled framework. This involves projection, separately, of the incoming and outgoing scattering wave functions on either the asymptotic (diabatic) or locally adiabatic channel states to obtain information on how the incoming flux, initially associated with a given internal state, redistributes itself as a function of the interparticle separation both as the particles approach, and, subsequently, as the particles recede. Although a log-derivative method[16-21] will be used to solve the CC equations, in which the scattering wave function is not determined explicitly, the desired information on the flux redistribution can be obtained from the log-derivative propagators themselves. The method summarized here is an extension of some ideas contained in several of our recent publications.[22-24]

The organization of the present article is as follows: In the next section we introduce several important concepts such as adiabatic basis and the asymptotic separation of incoming and outgoing fluxes. In Sec. III we discuss how the linear-reference, log-derivative propagation scheme of Alexander and Manolopoulos[21] can be used to determine in each sector the fluxes associated with the incoming and outgoing waves. Then, in Sec. IV, we show that the separation of flux into incoming and outgoing components, which is valid asymptotically, continues to be valid as the collision partners approach. In Sec. V we present a simple stabilization procedure which prevents any locally closed channels (in which the net flux must go rapidly to zero) from contaminating the flux propagation for locally open channels. Then follow three demonstrations of the technique: In Sec. VI for a pedagogical two-state problem, in Sec. VII for a multistate collision system involving four different electronic potential curves, and in Sec. VIII for a second multistate collision system involving a closed-channel resonance. We close with a brief conclusion.

 0021-9606/91/248931-10$03.00

II. CLOSE-COUPLED EQUATIONS

The general structure of the close-coupled equations can be expressed by the matrix equation

$$[\mathbf{1}d^2/dR^2 + \mathbf{W}(R)]\mathbf{F}(R) = 0. \tag{1}$$

Here R designates the interparticle separation, $\mathbf{1}$ is the identity matrix, and the matrix $\mathbf{W}(R)$ includes the (full, symmetric) matrix of the coupling potential as well as the diagonal matrices of the centrifugal potential (for gas-phase collisions) and the translational energy associated with each internal state (channel). This $\mathbf{W}$ matrix is expressed in a basis which is the product space of the internal states of the isolated collision partners, which we denote as $|\mathbf{d}\rangle$. Alternatively, a fully adiabatic basis $|\mathbf{a}\rangle$ can be defined,[25,26] by an orthogonal transformation of the diabatic basis, as

$$|\mathbf{a}\rangle = \mathbf{T}(R)|\mathbf{d}\rangle. \tag{2}$$

The transformation matrix is chosen to diagonalize the matrix of the total Hamiltonian

$$\mathbf{T}(R)\mathbf{W}(R)\mathbf{T}^T(R) = \boldsymbol{\lambda}(R) \equiv -\mathbf{k}^2(R), \tag{3}$$

where $\boldsymbol{\lambda}(R)$ is the (diagonal) matrix of eigenvalues and $\mathbf{k}^2(R)$ is the diagonal wave-vector matrix. Asymptotically, the j th element of this matrix is just the wave vector associated with the j th channel, namely

$$\lim_{R\to\infty} [\mathbf{k}^2(R)]_j = k_j^2 \equiv (2\mu/\hbar^2)(E - \epsilon_j), \tag{4}$$

where μ is the collision reduced mass and ϵ_j designates the internal energy.

Asymptotically, the solutions which are regular at the origin satisfy the boundary conditions (for inelastic collisions)

$$\lim_{R\to\infty} \mathbf{F}(R) = \mathbf{I}(R) + \mathbf{O}(R)\mathbf{S}, \tag{5}$$

where $\mathbf{S}$ designates the scattering matrix and $\mathbf{I}$ and $\mathbf{O}$ are diagonal matrices with elements proportional to Ricatti–Hankel functions, which are sums of the real Ricatti–Bessel functions of the first kind,[27] namely

$$[\mathbf{I}(R)]_{jk} = -i\delta_{jk}\hat{h}_l^{(2)}(k_jR) \equiv k_j^{-1/2}[j_l(k_jR) - iy_l(k_jR)], \tag{6a}$$

and

$$[\mathbf{O}(R)]_{jk} = -i\delta_{jk}\hat{h}_l^{(1)}(k_jR) \equiv k_j^{-1/2}[j_l(k_jR) + iy_l(k_jR)], \tag{6b}$$

with l denoting the orbital angular momentum of the collision pair in channel j. Although this angular momentum will, in general, differ from channel to channel, for notational simplicity we shall suppress any channel subscript on the orbital angular momentum, unless necessary. Since[27]

$$\lim_{R\to\infty} \hat{h}_l^{(1)}(k_jR) = -ik_j^{-1/2}\exp[i(k_jR - l\pi/2)] \tag{7}$$

and

$$\lim_{R\to\infty} \hat{h}_l^{(2)}(k_jR) = ik_j^{-1/2}\exp[-i(k_jR - l\pi/2)], \tag{8}$$

the boundary conditions in Eq. (5) are completely equivalent to the usual expression[3] in terms of $\exp[\pm i(k_jR - l\pi/2)]$.

As is clear from Eq. (5), the k th column of the solution matrix $\mathbf{F}(R)$ represents the expansion over the set of internal states of the scattering wave function corresponding to incoming flux in the k th internal state. We can without loss of generality break $\mathbf{F}(R)$ apart as

$$\mathbf{F}(R) = \mathbf{F}_i(R) + \mathbf{F}_o(R), \tag{9}$$

where the subscripts designate incoming and outgoing waves and

$$\lim_{R\to\infty} \mathbf{F}_i(R) = \mathbf{I}(R) \tag{10a}$$

and

$$\lim_{R\to\infty} \mathbf{F}_o(R) = \mathbf{O}(R)\mathbf{S}. \tag{10b}$$

At this point we shall define a *flux matrix* $\mathbf{J}(R)$ whose jk th element is the flux (current density) in internal state j at internuclear separation R, corresponding to incoming flux of magnitude $\hbar/\mu$ in internal state k, namely

$$[\mathbf{J}(R)]_{jk} = (i\hbar/2\mu)[\mathbf{F}(R)\cdot\mathbf{F}'(R)^* - \text{c.c.}]_{jk}. \tag{11}$$

Here $\mathbf{F}'$ designates the first derivative of the solution matrix with respect to R and the multiplication is taken to mean element-by-element multiplication rather than a matrix product. Obviously,

$$\lim_{R\to\infty} [\mathbf{J}(R)]_{jk} = (\hbar/\mu)(-\delta_{jk} + |S_{jk}|^2). \tag{12}$$

Formally, one can separate the flux into incoming and outgoing components

$$\mathbf{J}(R) = \mathbf{J}_i(R) + \mathbf{J}_o(R), \tag{13}$$

where

$$\lim_{R\to\infty} [\mathbf{J}_i(R)]_{jk} = -\hbar\delta_{jk}/\mu \tag{14a}$$

and

$$\lim_{R\to\infty} [\mathbf{J}_o(R)]_{jk} = \hbar|S_{jk}|^2/\mu. \tag{14b}$$

Our definition of the flux [Eq. (11)] is consistent with the convention that a *negative* sign corresponds to flux directed inward (toward decreasing R).

It is clear from Eqs. (5), (6), and (9) that as $R\to\infty$, the incoming and outgoing flux can be determined solely in terms of the incoming and outgoing waves, namely

$$\lim_{R\to\infty} [\mathbf{J}_i(R)]_{jk} = (i\hbar/2\mu)[\mathbf{F}_i(R)\cdot(d/dR)\mathbf{F}_i(R)^* - \text{c.c.}]_{jk}, \tag{15}$$

with a similar equation for the outgoing flux. It is intuitively appealing that this separation would persist as the value of R decreases; in other words that the flux associated initially with the incoming wave could be determined solely from the incoming wave at all values of R, and similarly for the flux associated with the outgoing wave, and that the *total* incoming or outgoing flux at any value of R is separately conserved. The demonstration that these claims are indeed valid

will be deferred to Sec. IV, below.

Equations (13) and (15) provide a powerful means for analysis of the collision dynamics: As the two particles approach, the progressive transfer of the initial flux associated with a particular internal state into the other internal states is a probe of the region of interparticle separation over which the collision effectively couples pairs of internal states. Similarly, examination of the outgoing flux, again as a function of the interparticle distance, gives information on how quickly the distribution among internal states relaxes into the asymptotic distribution, as would be determined in a conventional CC calculation. We believe that it is physically more meaningful to examine the redistribution of flux in the *adiabatic* basis, since the adiabatic states are the local eigenstates of the system, as a function of the interparticle separation. Transfer of flux between adiabatic states is a measure of the extent to which the collision occurs too quickly for the system to follow adiabatically. The determination of the fluxes in the adiabatic basis can be achieved by applying the transformation of Eq. (2) to the wave function and its derivative before the calculation of the flux matrix. The determination of the incoming and outgoing fluxes in the either basis can be implemented as a relatively simple extension of an available algorithm for solution of the CC equations. This will be described in the following section.

III. DETERMINATION OF STATE FLUXES

Solution of the CC equations involves numerical propagation of a set of N linearly independent solutions outward from a value of R small enough that all the internally states are classically inaccessible (closed).[3] In practice, this is done by breaking up the range of integration into a number of sectors, and defining an algorithm for propagation across each sector. One of the most stable and efficient of these algorithms, introduced originally by Johnson,[16] is based on the use of log-derivative propagators.[3,16–19,21,28] In this technique the wave function and its derivative at either side of each sector are related by

$$\begin{bmatrix} \mathbf{F}'(R_{m-1}) \\ \mathbf{F}'(R_m) \end{bmatrix} = \begin{bmatrix} \mathbf{L}_1^{(m)} & \mathbf{L}_2^{(m)} \\ \mathbf{L}_3^{(m)} & \mathbf{L}_4^{(m)} \end{bmatrix} \begin{bmatrix} -\mathbf{F}(R_{m-1}) \\ \mathbf{F}(R_m) \end{bmatrix}, \quad (16)$$

where R_{m-1} and R_m define the sides of sector m with $R_{m-1} < R_m$. In Eq. (16) each of the log-derivative propagators $\mathbf{L}_i^{(m)}$ is a matrix of dimension equal to the number of channels. For problems involving real potentials,[20]

$$\mathbf{L}_3^{(m)} = \mathbf{L}_2^{(m)T}. \quad (17)$$

We shall assume Eq. (17) to be valid here. In practice, in any log-derivative based solution of the CC equations, it is necessary to determine these four propagators, although the S matrix is obtained solely from the asymptotic form of the logarithmic derivative of the solution vector

$$\mathbf{Y}(R) = \mathbf{F}'(R)\mathbf{F}(R)^{-1}. \quad (18)$$

Solution of the CC equations involves stepwise propagation of the log-derivative matrix into the asymptotic region. Simultaneously with this propagation, one can determine, and store, the log-derivative propagators in each sector. This is particularly convenient in the case of a "potential following" method.[3,21,29,30] Here, the Hamiltonian matrix $\mathbf{W}(R)$ in Eq. (1) is diagonalized at the midpoint of each sector. By analogy to Eq. (3), we shall designate by $\mathbf{T}_m$ the corresponding transformation matrix for sector m. After transformation, the CC equations in the sector are diagonal, if one ignores the (presumably small) off-diagonal coupling, and the log-derivative propagators $\mathbf{L}_i^{(m)}$ are diagonal matrices, which, in the case of a linear reference potential, can be expressed in terms of Airy functions and their derivatives.[21] Often one stores the sector transformation matrices $\mathbf{T}_m$ in preparation for calculations at additional values of the total energy. For determination of the fluxes it is necessary to store, in addition, only the three diagonal propagators $\mathbf{L}_i^{(m)}$ $(i = 1,2,4)$.

From Eq. (16) one can show that the solution matrix at the left-hand side of the sector is given in terms of its value and its derivative at the right-hand side by

$$\mathbf{F}(R_{m-1}) = -[\mathbf{L}_3^{(m)}]^{-1}[\mathbf{F}'(R_m) - \mathbf{L}_4^{(m)}\mathbf{F}(R_m)]. \quad (19a)$$

With Eqs. (16) and (18) the derivative at the left-hand side can be obtained directly as

$$\mathbf{F}'(R_{m-1}) = -\mathbf{L}_1^{(m)}\mathbf{F}(R_{m-1}) + \mathbf{L}_2^{(m)}\mathbf{F}(R_m). \quad (19b)$$

After determination of the S matrix, the wave function and its derivative, and, subsequently, the flux [from Eq. (11)], can be calculated from Eq. (19) at each sector boundary. This procedure is carried out in steps, progressing inwards from the outermost value of R. This involves (1) transforming the wave function at the outer boundary of the sector into the locally adiabatic basis using the sector transformation matrix $\mathbf{T}_m$, (2) using Eq. (19) to determine the wave function and its derivative at the inner boundary of the sector (still in the locally adiabatic basis), (3) transforming the wave function at the inner boundary into the asymptotic basis using the transpose of the sector transformation matrix, and (4) determining the flux at the inner boundary from Eq. (11). Determination of the flux in the locally adiabatic rather than asymptotic basis can be achieved by inverting steps (3) and (4).

The computational effort involved in the determination of the flux will scale as $2N_i \times N_{\rm ch}^2$, where N_i is the number of initial states from which one wishes to follow the flux redistribution and $N_{\rm ch}$ is the number of channels. Since N_i will usually be significantly less than $N_{\rm ch}$, we see that the computational effort will be much less than that associated with the original solution of the CC equations, which scales as $N_{\rm ch}^3$.[30,31] The additional I/O overhead will involve $N_{\rm ch}^2 + 3N_{\rm ch}$ floating-point writes per sector. Buffering can be used to minimize the time spent on I/O.

IV. CONSERVATION OF FLUXES

Although asymptotically the net flux can rigorously be separated into the sum of an incoming and outgoing component [Eq. (5)], it might be argued that this separation could break down as the wave functions are propagated inward; that, for example, the purely incoming wave would pick up an outgoing component due to partial reflection at the sector boundaries. This would confound the mechanistic implications of the compound fluxes associated, separately, with the

asymptotically incoming and asymptotically outgoing waves. In this section we shall show that this apprehension is groundless.

The first argument is the demonstration that the magnitude and sign of the incoming (or outgoing) flux associated with each locally adiabatic state is preserved during propagation through a given sector. The proof is as follows.

The demonstration is easiest in terms of the Cauchy, rather than log-derivative propagators, which are defined, in analogy with Eq. (16) as[3,17,20]

$$\begin{bmatrix} \mathbf{F}(R_{m-1}) \\ \mathbf{F}'(R_{m-1}) \end{bmatrix} = \begin{bmatrix} \mathbf{C}_1^{(m)} & \mathbf{C}_2^{(m)} \\ \mathbf{C}_3^{(m)} & \mathbf{C}_4^{(m)} \end{bmatrix} \begin{bmatrix} \mathbf{F}(R_m) \\ \mathbf{F}'(R_m) \end{bmatrix}. \tag{20}$$

Since in each locally adiabatic sector the coupled equations are uncoupled, the corresponding Cauchy propagators are diagonal matrices, so that, within a locally adiabatic sector

$$\begin{bmatrix} \mathbf{f}(R_{m-1}) \\ \mathbf{f}'(R_{m-1}) \end{bmatrix} = \begin{bmatrix} \mathbf{c}_1^{(m)} & \mathbf{c}_2^{(m)} \\ \mathbf{c}_3^{(m)} & \mathbf{c}_4^{(m)} \end{bmatrix} \begin{bmatrix} \mathbf{f}(R_m) \\ \mathbf{f}'(R_m) \end{bmatrix}. \tag{21}$$

Here, the lower case letters are used to designate the diagonal character of the local Cauchy propagators $\mathbf{c}_i^{(m)}$. In addition, since we are implicitly propagating a single column of the solution matrix, corresponding to flux in a single initial state, we shall use lower case $\mathbf{f}$ to designate the solution (and its derivative) which are column vectors, rather than the upper-case notation Secs. II and III, which refers to the full $N \times N$ solution matrix. From Eq. (21) one can show that

$$[\mathbf{j}(R_{m-1})]_j = [\mathbf{c}_1^{(m)}\mathbf{c}_4^{(m)} - \mathbf{c}_2^{(m)}\mathbf{c}_3^{(m)}]_j [\mathbf{j}(R_m)]_j, \tag{22}$$

where

$$\mathbf{j}(R_m) = (i\hbar/2\mu)[\mathbf{f}(R_m)\cdot\mathbf{f}'(R_m)^* - \text{c.c}], \tag{23}$$

and similarly for $\mathbf{j}(R_{m-1})$. Since[21]

$$\mathbf{c}_1\mathbf{c}_4 - \mathbf{c}_2\mathbf{c}_3 = \mathbf{1}, \tag{24}$$

it follows that the fluxes (incoming, outgoing, or net) associated with each locally adiabatic state are preserved during propagation across a sector. Thus, the individual adiabatic channel components of the flux associated with either the incoming or outgoing waves at the outer (large R) boundary of a sector are not lost by back reflection with in the sector.

Furthermore, back reflection of the fluxes associated with either the asymptotically incoming or asymptotically outgoing waves does not occur during the transformation from one locally adiabatic sector into the next. To demonstrate this we shall show that the *total* flux (the flux summed over all internal states) associated with either the incoming or outgoing waves is preserved during propagation out of one locally adiabatic sector into the next.

Let $\mathbf{T}_m$ and $\mathbf{T}_{m-1}$ designate the transformation matrices into the locally adiabatic bases in sectors m and $m-1$, respectively, and $\mathbf{f}_m(R)$ and $\mathbf{f}_{m-1}(R)$ designate the locally adiabatic wave functions in these two sectors. The total flux at the inner (small R) boundary of sector m is

$$J_m(R_{m-1}) = (i\hbar/2\mu)\sum_j \{[\mathbf{f}_m(R)]_j \times [\mathbf{f}'_m(R)]_j^* - \text{c.c.}\}. \tag{25}$$

In matrix notation, this equation can be written more compactly as

$$J_m(R_{m-1}) = (i\hbar/2\mu)[\mathbf{f}_m(R_{m-1})^T \times \mathbf{f}'_m(R_{m-1})^* - \text{c.c.}]. \tag{26}$$

Now the locally adiabatic wave function at the outer (large R) boundary of sector $m-1$ is related to the wave function at the (common) inner boundary of sector m by

$$\mathbf{f}_{m-1}(R_{m-1}) = \mathbf{T}_{m-1}\mathbf{T}_m^T\mathbf{f}_m(R_{m-1}), \tag{27}$$

and similarly for the derivative. Thus the total flux at the outer boundary of sector $m-1$ is

$$\begin{aligned} J_{m-1}(R_{m-1}) &= (i\hbar/2\mu)[\mathbf{f}_{m-1}(R)^T\mathbf{f}'_{m-1}(R)^* - \text{c.c.}] \\ &= (i\hbar/2\mu)[\mathbf{f}(R_{m-1})^T\mathbf{T}_m\mathbf{T}_{m-1}^T\mathbf{T}_{m-1} \\ &\quad \times \mathbf{T}_m^T\mathbf{f}'_m(R_{m-1})^* - \text{c.c.}]. \end{aligned} \tag{28}$$

Since the transformation from the diabatic to adiabatic basis is orthogonal, Eq. (28) simplifies to

$$\begin{aligned} J_{m-1}(R_{m-1}) &= (i\hbar/2\mu)[\mathbf{f}_m(R)^T\mathbf{f}'_m(R)^* - \text{c.c.}] \\ &= J_m(R_{m-1}). \end{aligned} \tag{29}$$

Thus the total flux, summed over all channels, is conserved during the passage from one locally adiabatic sector to the next.

From Eq. (12) we observe that asymptotically, as $R \to \infty$, the total *incoming* flux is just $-\hbar/\mu$. The total *outgoing* flux is

$$(\hbar/\mu)\sum_j |S_{jk}|^2. \tag{30}$$

Because of the unitarity of the S matrix, the sum in Eq. (30) equals unity, so that asymptotically, the total *outgoing* flux is just $\hbar/\mu$, the negative of the total incoming flux. The argument earlier in this section implies then that, as R decreases, the total incoming and outgoing fluxes remain equal to, respectively, $\mp\hbar/\mu$. This latter argument holds provided that none of the asymptotically open channels become closed. The modifications in the presence of closed channels will be discussed in the next section.

V. STABILIZATION IN THE PRESENCE OF CLOSED CHANNELS

During the inward propagation of the wave function and its derivative, when one (or more) of the channels become closed, the exponentially growing component in the wave function begins to contaminate the wave function of the other open channels leading to unphysically large fluxes. In practice, a simple stabilization procedure can be invoked, as follows: In an adiabatic representation, *net* flux initially present in any channel goes rapidly to zero as the channel enters a classically forbidden region. To force this behavior, for any channel which is locally closed, in other words with $k_j^2(R_m) < 0$, the wave function and its derivative at the inner boundary of the sector (R_{m-1}) are damped according to the relation

$$f_j(R_{m-1}) \equiv [\mathbf{f}(R_{m-1})]_j = \zeta_j f_j^\circ(R_{m-1}), \tag{31}$$

where $f_j^o(R_{m-1})$ indicates the value which would have been predicted using the exact propagator relation, Eq. (19a). A simple, yet physically reasonable, choice of the damping function ζ_j can be made by assuming a constant potential in the sector in question. In this case

$$\zeta_j = \exp(-\alpha^{(m)}|\lambda_j^{(m)}|^{1/2}\Delta_m) = \exp(-|k_j^{(m)}|\Delta_m), \tag{32}$$

where $\lambda_j^{(m)}$ denotes the jth adiabatic eigenvalue in sector m, $k_j^{(m)}$ denotes the wave vector of adiabatic level j in sector m, $\alpha^{(m)}$ is a constant, and Δ_m denotes the width of sector m.

To follow the redistribution of flux when one (or more) of the classically allowed channels penetrates through a low barrier, the damping correction can be introduced whenever $k_j^2(R_m)$ is less than a suitably chosen negative value.

Since the flux associated with the adiabatic channel which has been damped drops rapidly to zero, for this channel the conservation of flux across the sector discussed in the preceding section is no longer valid. Thus, the component of the flux in each adiabatic channel is conserved during propagation across a sector, without back reflection, but only *as long as the channel remains open*. Furthermore, because flux in a particular adiabatic channel is eliminated once the channel is closed, during the transformation out of sector m, say, into sector $m-1$ the conservation of *total* flux, discussed in the preceding section, will apply only to the sum of the fluxes associated with those channels which are still open at the inner (small R) boundary of sector m. One might then argue that during the transformation from sector m into sector $m-1$, flux associated with adiabatically open channels will become transferred into adiabatically closed channels and, hence, become artificially lost because the latter are damped out by Eq. (31). Because energetically closed states will make only an exponentially small contribution to the adiabatic wave functions, this loss of flux will be similarly small. The extent of the errors introduced in a representative case will be explored in more detail in Sec. VIII.

VI. DEMONSTRATION: TWO-STATE PROBLEM

The first demonstration of the method presented here for the quantum study of the redistribution of inelastic flux will be a pedagogical two-state problem, involving the crossing of two potentials, the first a Morse potential

$$V_1(R) = 0.5\exp[-0.4(R-6.5)] \times\{\exp[-0.4(R-6.5)]-2\} \tag{33}$$

and the second, a shifted exponential

$$V_2(R) = 100\exp(-0.8R) - 1, \tag{34}$$

with energy in millihartree and distance in bohr. These two curves are coupled by the potential

$$V_{12}(R) = 0.2\exp[-0.5(R-4.2)]. \tag{35}$$

The resulting adiabatic potential curves are shown in Fig. 1. Let us consider collisions in which the system is originally in state $|1\rangle$, and enters on the upper of the two curves shown in Fig. 1. Of interest will be the probability for transition to the second state $|2\rangle$, with the particles separating on the lower of the two curves shown in Fig. 1. A simple semiclassical analysis[25,26] predicts that this transition will occur primarily at the avoided crossing between the two curves, which is centered at $R = 6.62$ bohr. Additionally, the transition probability will oscillate as a function of energy, which is a consequence of interference between trajectories which undergo this nonadiabatic crossing as the particles approach and as they recede. This is seen in Fig. 2, which displays the $1\rightarrow 2$ transition probability over a range of collision energies for a collision mass of 42 a.m.u.

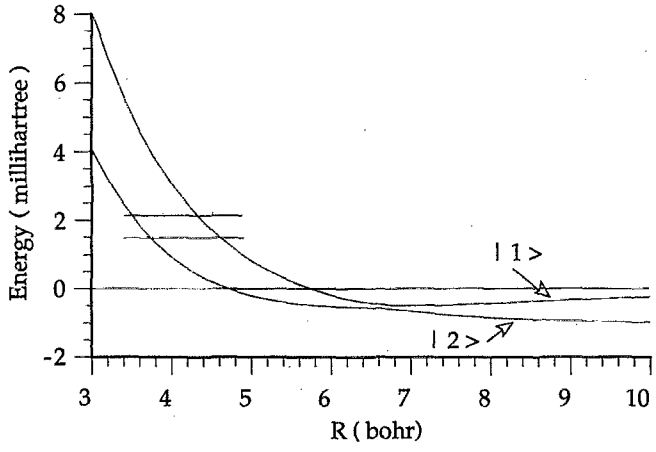

FIG. 1. Adiabatic potential energy curves for the two-state model problem described (Sec. IV) by Eqs. (33)–(35). The underlying diabatic curves cross at $R = 6.62$ bohr. The horizontal lines indicates the value of the total energy (336 and 472 cm^{-1}) used in the flux calculations described in Sec. VI and in Figs. 3 and 4.

Figure 3 displays the incoming and outgoing fluxes in the upper and lower adiabatic states as a function of distance for $E = 336$ cm^{-1}, which corresponds to the maximum in the transition probability curve in Fig. 2. Initially, only the upper state is assumed populated. For illustrative purposes, we associate the incoming flux with negative distances and the outgoing flux, with positive distances. In addition, although the incoming flux is negative (by definition), for il-

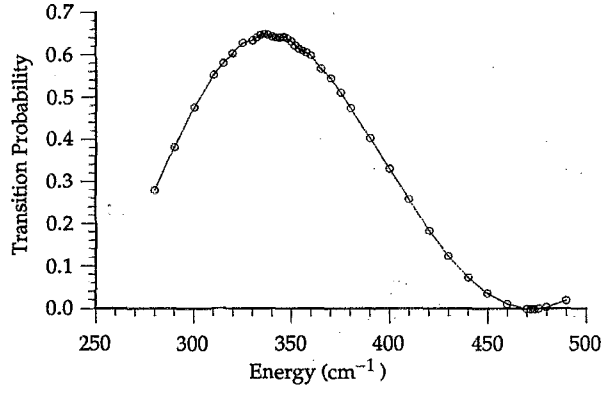

FIG. 2. Transition probabilities from the upper state $|1\rangle$ to the lower state $|2\rangle$ as a function of total energy for the two-state system described by Eqs. (33)–(35) and illustrated in Fig. 1. The reduced mass of the collision partners was taken, arbitrarily, to be 42 a.m.u. The slight structure in the curve near the maximum is reproducible and does not appear to be attributable to numerical error in the integration of the CC equations.

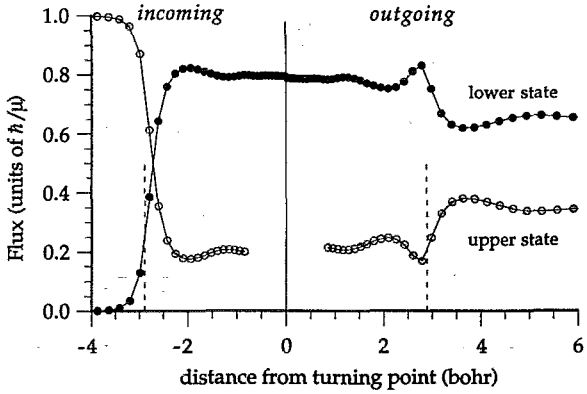

FIG. 3. Illustration of the incoming and outgoing flux associated with the *adiabatic* states in Fig. 1 as a function of the interparticle separation, for the model two-state problem described by Eqs. (33)–(35) and a collision energy of 336 cm^{-1}. At this energy the probability for transition from the upper to lower state is maximal (Fig. 2). The initial incoming flux is entirely in the upper state. (Solid circles) flux in the lower adiabatic state; (open circles) flux in the upper adiabatic state. The fluxes are plotted as a function of the distance from the turning point of the upper adiabatic curve (Fig. 1), which is 3.73 bohr at this energy. To illustrate in a more pictorial manner the evolution of the collision, the coordinate associated with the incoming flux is plotted as a negative, and the sign of the incoming flux itself, which is a negative number, has been reversed. The location of the curve crossing, at $R = 6.62$ bohr, is indicated by the vertical dashed lines.

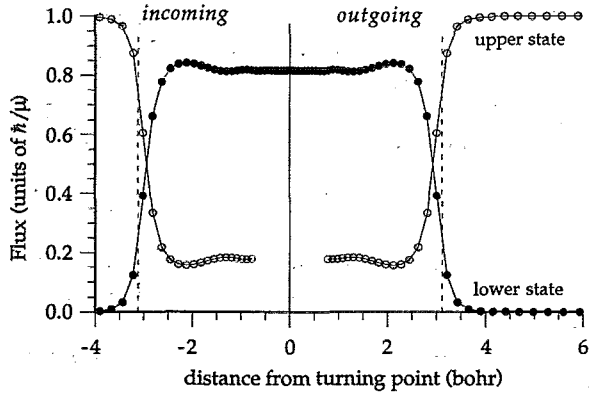

FIG. 4. Illustration of the incoming and outgoing flux associated with the *adiabatic* states in Fig. 1 as a function of the interparticle separation, for the model two-state problem described by Eqs. (33)–(35) and a collision energy of 472 cm^{-1}. At this energy the probability for transition from the upper to lower state is effectively zero (Fig. 2). The initial incoming flux is entirely in the upper state. (Solid curves) flux in the lower adiabatic state; (open circles) flux in the upper adiabatic state. The fluxes are plotted as a function of the distance from the turning point of the upper adiabatic curve (Fig. 1), which is 3.50 bohr at this energy. To illustrate in a more pictorial manner the evolution of the collision, the coordinate associated with the incoming flux is plotted as negative, and the sign of the incoming flux itself, which is a negative number, has been reversed. The location of the curve crossing, at $R = 6.62$ bohr, is indicated by the vertical dashed lines.

lustrative purposes the incoming flux is plotted in Fig. 3 as a positive quantity. The calculated fluxes are plotted as a function of the distance from the classical turning point on the inner adiabatic potential ($R_c = 3.73$ bohr). The flux associated with the upper state is plotted only for distances outside of the classical turning point associated with this state ($R_c = 4.60$ bohr). Figure 3 illustrates the gradual transfer of flux from the upper adiabatic state to the lower as the particles approach and then, as they recede. As would be anticipated by a semiclassical analysis, flux transfer is virtually nonexistent until the two particles reach the curve crossing. We also observe a definite asymmetry in the collision: As the particles recede beyond the crossing point, flux transfer continues to a far greater extent than seen in the initial approach. The slight discontinuity between the incoming and outgoing fluxes at the classical turning point is a measure of the degree of error introduced by the simple stabilization procedure introduced in Sec. V.

Figure 4 presents a similar view of the flux redistribution in the adiabatic basis, for at a collision energy of 472 cm^{-1}, where the transition probability from the upper to the lower states fall to zero (Fig. 2). As one might have anticipated, we see that at this energy the collision is perfectly symmetric: The flux transfer from the upper to the lower state which occurs as the partners approach is exactly reversed as they recede.

VII. DEMONSTRATION: MULTISTATE PROBLEM

As a second demonstration of the power of this new technique for the study of flux redistribution during a collision, we shall examine inelastic collisions of Ca($4s4p^2P$) with a He atom. This system has been the focus of much recent theoretical interest in our group,[23,24,32–34] with motivation by the concurrent experimental study in the group of Leone at the Joint Institute for Laboratory Astrophysics.[35–40] For details of the theoretical description of the interaction and subsequent collisions we refer the reader to the earlier work of Pouilly and Alexander.

The calculations to be described used the $^{1,3}\Pi$ and $^{1,3}\Sigma$ Ca–He potential curves given by Pouilly *et al.*[34] and were carried out at an initial energy in the ^1P state of 540 cm^{-1} and a total angular momentum of $J_{tot} = 10$. The six adiabatic potential curves associated with the f labeled levels[23,33,41] are shown in Fig. 5. The dominant spin–orbit mixing involves the $^1\Pi_{1f}$ and $^3\Sigma_{1f}$ states, which correlate asymptotically with the $^1P_{1f}$ and $^3P_{2f}$ levels, respectively. Note that there is no direct spin–orbit coupling between the singlet state and the $^3\Sigma_{10}$ state (Refs. 23, 33, and 34) since the selection rule for the spin–orbit operator is $\Delta\Omega = 0$ (Refs. 42 and 43) Fig. 5 indicates the avoided crossing between the $^1\Pi_{1f}$ and $^3\Sigma_{1f}$ curves, as well as the region of "radial coupling" (Refs. 26, 44, and 45), at which point the splitting between the $^3\Sigma$ and ^3P curves becomes comparable to the fine structure splittings in the ^3P state of the isolated Ca atom [7 cm^{-1} between the $^3P_0$ and $^3P_1$ levels and 28 cm^{-1} between the $^3P_1$ and $^3P_2$ levels (Ref. 46)].

Partial cross sections for transitions from the $^1P_{1f}$ to the $^3P_{J=0,1,2}$ levels, summed over the projection degeneracy of the final state, are displayed in Fig. 6. As in Fig. 2, the pronounced oscillatory structure in the partial cross sections is a manifestation of Stückelberg oscillations between trajectories which undergo the singlet→triplet crossing as the particles approach and as they recede.

Figure 7 displays the incoming and outgoing flux corre-

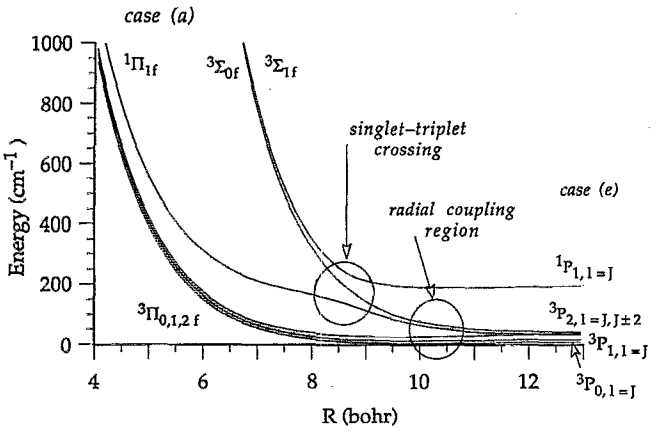

FIG. 5. Dependence on internuclear distance of the six f labeled adiabatic potential curves for the collision of Ca($4s4p^{1,3}P$) with He for $J_{tot} = 10$. The curves are designated by appropriate Hund's case (a) and case (e) labeling (valid at small and large R, respectively, see Refs. 23 and 34). The underlying electronic potential curves were taken from Ref. 34. The region of strong spin–orbit mixing between the $^1\Pi_{1f}$ and $^3\Sigma_{1f}$ curves is shown, as is the region of "radial coupling" (Refs. 26, 44, and 45) at which point the splitting between the $^3\Sigma$ and ^3P curves becomes comparable to the fine structure splittings in the ^3P state of isolated Ca atom.

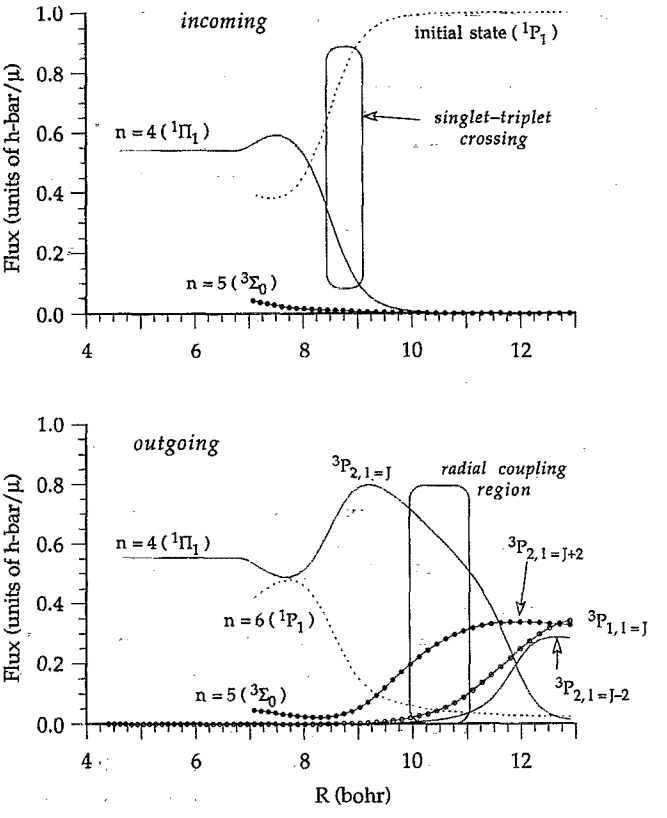

FIG. 7. (Upper panel) Incoming flux in the various adiabatic f labeled states of the Ca($4s4p^{1,3}P$) He system (see Fig. 5) at an energy in the ^1P state of 540 cm^{-1} and $J_{tot} = 10$. The fluxes in the various adiabatic states are plotted only up to the classical turning points for these states. The initial state, with flux indicated by the dashed curve, is $n = 6(^1P_{1f})$. The incoming flux in the $n = 1$, 2, and 3 states is negligibly small on the scale of the figure. (Lower panel) Identical to the upper panel except that the outgoing flux is plotted. The outgoing flux in the $^3P_{0f}$ state ($n = 1$) is found to be negligibly small.

sponding to initial excitation of the $^1P_{1f}$ state for $J_{tot} = 10$ and $E_{col} = 540$ cm^{-1}. As can be seen in Fig. 6, this value of J_{tot} corresponds to a local maximum in the partial cross sections for singlet-triplet transfer. As one might anticipate from the adiabatic energy curves in Fig. 5, transfer of flux out of the initial state occurs almost exclusively to the $n = 4$ state, which is the only state which is directly coupled with the initial state by the spin–orbit operator. By contrast, as anticipated earlier, only relatively little flux transfer occurs to the $n = 5$ state, since this state correlates with the Hund's case (a) $^3\Sigma_{0f}$ state which is not directly coupled with the $^1\Pi_{1f}$ state.

The corresponding outgoing flux is displayed in the lower panel of Fig. 7. We see that the transfer of flux from the ^1P to the $n = 4$ (triplet) state occurs roughly equally as the particles approach and as they recede. More remarkably, the $n = 4$ triplet state, which is dominantly populated initially, loses almost all its flux to other $^3P_2$ and $^3P_1$ states as the particles recede through the "radial coupling" region. We also observe the virtual absence of flux transfer from the $^1P_{1f}$ state into the $^3P_0$ state. In the molecular region the $^3P_0$ state correlates with the $^3\Pi_0$ state (see Fig. 5), which is not directly coupled to the initially populated $^1\Pi_{1f}$ state. Thus, as discussed by Pouilly *et al.*,[34] population of the $^3P_0$ state will occur only through second-order coupling involving the molecular states which correlate with the $^3P_{J=1,2}$ atomic states.

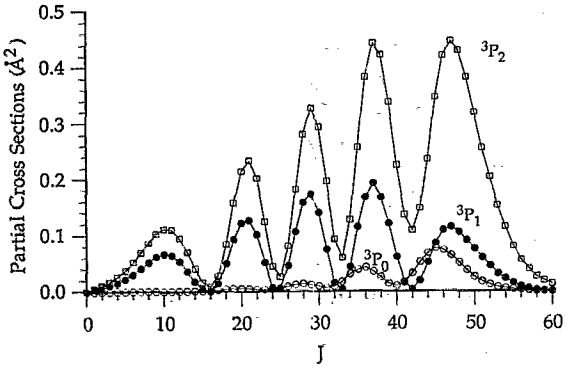

FIG. 6. Partial cross sections for scattering from the $^1P_{1f}$ state of Ca($4s5p$) into the three ^3P_J states of the same electron occupancy in collisions with He at an energy in the ^1P state of 540 cm^{-1}. The underlying adiabatic potential curves are shown in Fig. 5.

VIII. DEMONSTRATION: MULTISTATE PROBLEM WITH CLOSED CHANNELS

To illustrate the efficacity of the damping procedure for stabilization in the presence of closed channels, introduced in Sec. V, we present as a third example a system involving propagation into a region in which one of the asymptotically closed channels becomes energetically open. The specific system chosen in the classic problem of rotational inelasticity in collisions of N_2 with Ar.[47] We assume a rigid N_2 molecule with the simple interaction potential

$$V(R,\theta) = V_0(R) + V_2(R)P_2(\cos\theta), \qquad (36)$$

where in the usual Jacobi coordinate system **R** is the vector connecting the Ar atom and the center of mass of the N_2 molecule and θ is the angle between **R** and the N_2 bond axis. The expansion coefficients in Eq. (36) were taken to be those of the model interaction potential first introduced by Pattengill and co-workers, namely[48] (in units of hartree for energy and bohr for distance)

$$V_0(R) = 83.05(\rho^{12} - 2\rho^6), \tag{37a}$$

$$V_2(R) = 83.05(0.5\rho^{12} - 0.26\rho^6), \tag{37b}$$

with

$$\rho = 7.4247/R. \tag{38}$$

We shall consider collisions at $J_{tot} = 0$ and an energy of 135 cm^{-1}, measured with respect to the $J = 0$ level of N_2. The adiabatic potential curves which correlate with the first five lowest rotational levels of o-N_2 ($J = 0$, 2, 4, 6, and 8) are illustrated in Fig. 8. We observe that at an energy of 135 cm^{-1} the $J = 8$ level, with a rotational energy of 144.7 cm^{-1}, is asymptotically closed, but becomes open for $R < 11.5$ bohr—a classic resonance. As the collision partners approach we might expect to see some flux transfer into the $n = 5$ ($J = 8$) level, which then becomes depopulated as the partners recede to beyond 11.5 bohr.

Without the introduction of the damping factor discussed above in Sec. V, the calculated incoming and, in a more pronounced manner, outgoing fluxes associated with either the open ($n = 0 - 4$) or closed ($n = 5$) levels become irretrievably contaminated by the exponentially growing term in the wave function associated with the closed channel. This is completely eliminated with the introduction of Eqs. (31) and (32). Here we used a correction factor $\alpha^{(m)} = 1.0$ in Eq. (32). The upper and lower panels of Fig. 9 illustrate, respectively, the incoming and outgoing fluxes associated with the adiabatic states $n = 1$, 2, 4, and 5 ($J = 0$, 2, 6, and 8) corresponding to incoming flux in $n = 3$ ($J = 4$). As in Figs. 4, 5, and 6 the fluxes are displayed only in the classically allowed region associated with each adiabatic state, where the concept of flux has a physical sense. Inside the classically forbidden regions, the flux vanishes exponentially.

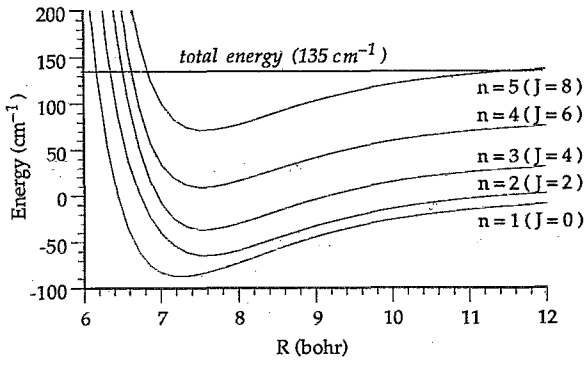

FIG. 8. Adiabatic potential curves for the collision of o-N_2 with Ar, for $J_{tot} = 0$ and functions of positive total parity, determined using the potential described in Eqs. (37) and (38). At a total energy of 135 cm^{-1} the adiabatic state which corresponds asymptotically to $N_2(J = 8)$ becomes open for $R < 11.5$ bohr.

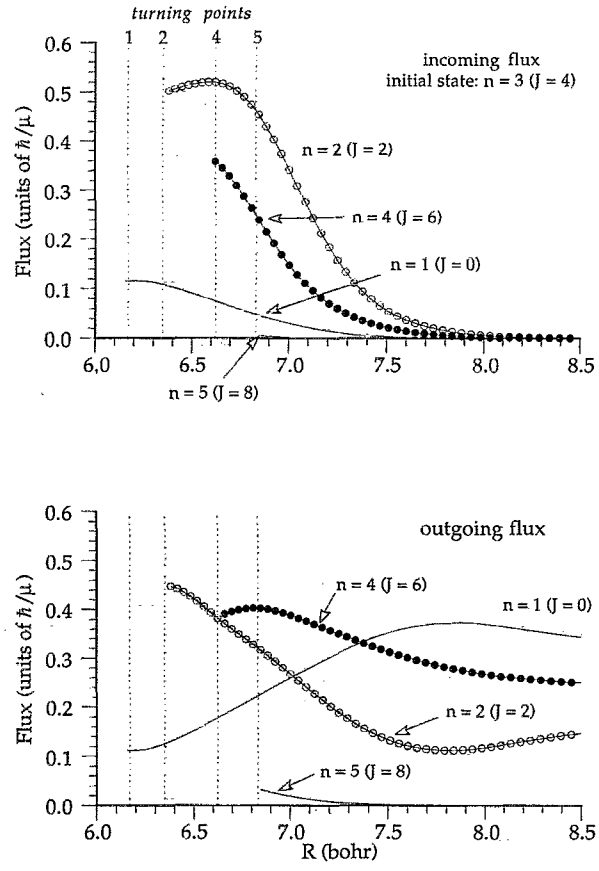

FIG. 9. (Upper panel) Incoming flux in the various adiabatic states for the collision of o-N_2 with Ar, at a total energy of 135 cm^{-1} and $J_{tot} = 0$. The corresponding adiabatic potential curves are shown in Fig. 8. Initially the N_2 molecule is in the $J = 4$ rotational level. The fluxes in the various adiabatic states are plotted only up to the classical turning points for these states, which are illustrated by dashed vertical lines. (Lower panel) Identical to the upper panel except that the *outgoing* flux is plotted.

We see clearly how flux appears in the asymptotically closed ($n = 5$) state, disappears as the state again becomes closed at $R = 6.82$ bohr, reappears as the particles then separate, and disappears again. We further observe that significant flux in the $n = 5$ state is confined only to a small region (6.8 bohr $< R <$ 7.5 bohr), although the outer turning point of this state occurs at much larger distances (see Fig. 8). In addition, we observe that the state which is first populated inelastically ($n = 2$) gains flux and dominates the distribution in the close range region but then gradually loses flux, primarily to the lowest ($n = 1$) state, as the particles recede.

As an adiabatic channel penetrates into a classically forbidden region, the component of the true wave function for this state becomes purely real, so that the flux associated with this state drops to zero. Although this is forced by the stabilization correction introduced in Sec. V, one might expect the incoming and outgoing fluxes associated with a given adiabatic state to become equal even before the state becomes classically closed. We see from Fig. 9 that this is not

strictly satisfied. In addition, in the small R region in which only the lowest ($n = 1$) state is open, the incoming and outgoing fluxes are not precisely identical, although, in principle, they should be equal, particularly if all the other adiabatic states are strongly forbidden. Figure 10 displays the *net* flux (that which correlates with the outgoing wave minus that which correlates with the incoming wave) for the $n = 1$ adiabatic state as a function of distance. As can be seen, in the region inside the classical turning point for the second adiabatic state ($n = 2$), the calculated net flux associated with $n = 1$ is small, but not quite zero. This discrepancy is certainly a measure of the magnitude of the error introduced by the simplistic stabilization correction introduced in Sec. V.

IX. DISCUSSION

We have presented here a new method for the fully quantum study of the dynamics of inelastic molecular collisions. This method is based on the determination, as a function of interparticle separation, of the redistribution of the incoming inelastic flux among the various internal quantum states of the system, which can refer to either an asymptotic (diabatic) or locally adiabatic expansion. Implementation involves inward propagation of the incoming and outgoing wave functions, the later determined in a prior solution of the close-coupled equations for the system under study, and the concomitant determination of the flux matrix. This propagation and flux determination (in either the asymptotic or locally adiabatic bases) can be done in a straightforward manner by employing the transformation matrices and diagonal log-derivative propagators which underlie our implementation[21] of the linear reference potential algorithm[29,20] for the solution of the CC equations. A simple damping correction was introduced to eliminate the numerical instabilities which accompany propagation into regions where some of the channels become closed. A particular advantage of the use of our linear reference potential algorithm is that the flux redistribution can be investigated in an adiabatic basis, which represents the natural eigenstates of the system as a function of interparticle distance.

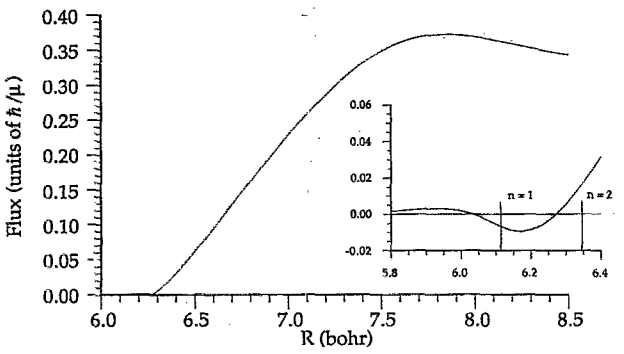

FIG. 10. Net flux (outgoing-incoming) in the lowest ($n = 1$) adiabatic state for the collision of o-N_2 with Ar, at a total energy of 135 cm^{-1} and $J_{tot} = 0$. The corresponding adiabatic potential curves are shown in Fig. 8. The inset panel provides greater detail. The vertical lines in the inset panel indicate the classical turning point for the two lowest ($n = 1$ and $n = 2$) adiabatic states.

Applications were made to a pedagogical two-state curve-crossing system, to a multichannel problem involving four coupled electronic potential curves, and to a multichannel collision at low energy involving a closed channel resonance. These studies revealed a wealth of interesting and often unexpected information about the redistribution of the initial flux during the course of the collision. In all cases we saw that the flux transfer during the collision was more dramatic than might be inferred from the final product distributions. As might have been anticipated, the flux redistribution calculations were seen to be in accord with simple qualitative predictions based on well-established semiclassical methods.[25,26] Additionally, the analysis showed a definite asymmetry in the collision process: relatively little flux transfer during the approach phase, with markedly greater inelasticity occurring as the particles receded.

We further concluded that the errors introduced by the simple stabilization correction introduced in Sec. V are small; a conservative estimate is on the order of a few percent of the total incoming flux. The primary usage of the technique, introduced here, for the study of the redistribution of collision flux will be *qualitative* analysis of collision mechanisms, rather than *quantitative* predictions of quantities which would be difficult (at best) to measure. We believe that this goal will not be affected by the small errors introduced by the stabilization correction for closed channels. Nevertheless, future work should certainly be directed to the development of more accurate ways of eliminating the numerical contamination due to closed channels.

To illustrate better the conceptual differences between the method presented here and the time-dependent close-coupled wave-packet method of Kouri and co-workers,[9–13] we make use of an experimental analogy. The present approach is equivalent to placing a series of detectors along the reaction path, which can measure the distribution of the system among the internal states which are locally energetically accessible. The detectors are unidirectional, in that they are sensitive to the internal state distributions either as the collision partners approach or as they recede. They are further flux, rather than number, detectors and operate in a continuous, rather than pulsed, mode. The detectors used in the CC-WP method, on the other hand, operate in a pulsed, rather than continuous mode, and measure the time evolution of an initially prepared distribution of internal states, both in coordinate space and in internal state space. Because the CC-WP state detectors operate in pulsed, rather than cw, mode, there is an intrinsic uncertainty in the correlation between the population distributions in coordinate and internal state space. On the other hand, the time-independent method presented here, although allowing an unambiguous correlation between the population distributions in coordinate and internal state space, offers no information on the time evolution of the internal state distributions. In this context we refer the reader to the illuminating discussion in the text by Messiah in which the author contrasts the wave-packet and wave-function description of simple one-dimensional scattering.[49] In Messiah's interpretation the wave function represents a statistical ensemble of a large number of particles moving both in both the $+x$ and $-x$ direction.

This picture is philosophically identical to the interpretation presented earlier in this paragraph.

Because both the time-independent method presented here and the time-dependent CC-WP method are fully quantum, they offer the possibility of an exact investigation of dynamics of inelastic collision processes, free from any ambiguities which might arise from the separation of classical and quantum degrees of freedom (as is made in impact parameter methods) or from the complete neglect of quantum degrees of freedom (as is done in classical trajectory studies). When carried out in addition to a more conventional close-coupled calculation of inelastic cross sections, the time-independent analysis of initial flux redistribution, presented here, can be accomplished with only a minor increment in computational effort. In most cases, this will be more than justified by the additional understanding of the underlying chemistry which can be obtained. We expect to pursue further applications to problems of current interest.

ACKNOWLEDGMENTS

This research was supported by the National Science Foundation, under Grant No. CHE-8917543, and by the U.S. Army Research Office, under Grant No. DAAL03-91-G-0129. The author wishes to thank Dr. David Manolopoulos and Professor William Miller for helpful discussions and the Alexander von Humboldt Foundation for a Senior U.S. Scientist award, during the tenure of which part of the work described here was carried out at the University of Bielefeld, Germany. He is grateful to Professor Hans-Joachim Werner for his support, under SFB 216 from the Deutsche Forschungsgemeinschaft, and encouragement during that time.

[1] A. Arthurs and A. Dalgarno, Proc. R. Soc. London Ser. A **256**, 540 (1960).
[2] W. A. Lester, Jr., Methods Comput. Phys. **10**,211 (1971).
[3] See, for example, D. Secrest, in *Atom-Molecule Collision Theory: A Guide for the Experimentalist*, edited by R. B Bernstein (Plenum, New York, 1979), p. 265.
[4] T. F. Moran, M. R. Flannery, and P. C. Cosby, J. Chem. Phys. **61**, 1261 (1974).
[5] T. F. Moran, K. J. McCann, M. Cobb, R. F. Borkman, and M. R. Flannery, J. Chem. Phys. **74**, 2325 (1981).
[6] A. E. DePristo, J. Chem. Phys. **78**, 1237 (1983).
[7] B. M. Rice, B. C. Garrett, P. K. Swaminathan, and M. H. Alexander, J. Chem. Phys. **90**, 575 (1989).
[8] For a good recent review, see R. Kosloff, J. Phys. Chem. **92**, 2087 (1988).
[9] Y. Sun, D. J. Kouri, D. W. Schwenke, and D. J. Truhlar, Comput. Phys. Commun. **63**, 51 (1991).
[10] R. C. Mowrey and D. J. Kouri, J. Chem. Phys. **84**, 6466 (1986).
[11] R. C. Mowrey, H. F. Bowen, and D. J. Kouri, J. Chem. **86**, 2441 (1987).
[12] Y. Sun, R. C. Mowrey, and D. J. Kouri, J. Chem. Phys. **87**, 339 (1987).
[13] Y. Sun and D. J. Kouri, J. Chem. Phys. **86**, 6140 (1988).
[14] D. Lemoine and G. C. Corey, J. Chem. Phys. **92**, 6175 (1990).
[15] D. Lemoine and G. C. Corey, J. Chem. Phys. **94**, 767 (1991).
[16] B. R. Johnson, J. Comput. Phys. **13**, 445 (1973).
[17] F. Mrugala and D. Secrest, J. Chem. Phys. **78**, 5954 (1983).
[18] F. Mrugala and D. Secrest, J. Chem. Phys. **79**, 5960 (1983).
[19] D. E. Manolopoulos, J. Chem. Phys. **85**, 6425 (1986).
[20] D. E. Manolopoulos, Ph.D. thesis, University of Cambridge, 1988.
[21] M. H. Alexander and D. E. Manolopoulos, J. Chem. Phys. **86**, 2044 (1987).
[22] M. H. Alexander, G. Parlant, and T. Hemmer, J. Chem. Phys. **91**, 2388 (1989).
[23] M. H. Alexander and B. Pouilly, J. Chem. Phys. **90**, 5373 (1989).
[24] B. Pouilly and M. H. Alexander, Chem. Phys. **145**, 191 (1990).
[25] M. S. Child, *Molecular Collision Theory*, 2nd ed. (Academic, New York, 1974).
[26] E. E. Nikitin and S. Y. Umanskii, *Theory of Slow Atomic Collisions* (Springer-Verlag, Berlin, 1984).
[27] M. Abramowitz and I. Stegun, Natl. Bur. Stand. Appl. Math. Ser. **55** (1965), Sec. 10.3.
[28] L. D. Thomas, M. H. Alexander, R. B. Walker, B. R. Johnson, W. A. Lester, J. C. Light, K. D. McLenithan, G. A. Parker, M. J. Redmon, T. G. Schmalz, and D. Secrest, J. Comput. Phys. **41**, 407 (1981).
[29] R. G. Gordon, J. Chem. Phys. **51**, 14 (1969).
[30] R. G. Gordon, Meth. Comput. Phys. **10**, 81 (1971).
[31] H. Rabitz, J. Chem. Phys. **63**, 5208 (1975).
[32] B. Pouilly, T. Orlikowski, and M. H. Alexander, J. Phys. B **18**, 1953 (1985).
[33] B. Pouilly and M. H. Alexander, J. Chem. Phys. **86**, 4790 (1987).
[34] B. Pouilly, J.-M. Robbe, and M. H. Alexander, J. Chem. Phys. **91**, 1658 (1989).
[35] M. O. Hale and S. R. Leone, J. Chem. Phys. **79**, 3352 (1983).
[36] M. O. Hale, I. V. Hetel, and S. R. Leone, Phys. Rev. Lett. **53**, 2296 (1984).
[37] W. Bussert, D. Neuschäfer, and S. R. Leone, J. Chem. Phys. **87**, 3833 (1987).
[38] W. Bussert and S. R. Leone, Chem. Phys. Lett. **138**, 276 (1987).
[39] R. W. Schwenz and S. R. Leone, Chem. Phys. Lett. **133**, 433 (1987).
[40] S. R. Leone, in *Selectivity in Chemical Reactions*, edited by J. C. Whitehead (Kluwer Academic, Dordrecht, 1988), p. 245.
[41] J. M. Brown, J. T. Hougen, K.-P. Huber, J. W. C. Johns, I. Kopp, H. Lefebvre-Brion, A. J. Merer, D. A. Ramsay, J. Rostas, and R. N. Zare, J. Mol. Spectrosc. **55**, 500 (1975).
[42] J. T. Hougen, Natl. Bur. Stand. (U.S.) Monogr. **115** (1970).
[43] H. Lefebvre–Brion and R. W. Field, *Perturbations in the Spectra of Diatomic Molecules* (Academic, New York, 1986).
[44] E. E. Nikitin, J. Chem. Phys. **43**, 744 (1965).
[45] E. E Nikitin, in *Chemische Elementarprozesse*, edited by H. Hartmann (Springer, Berlin, 1968).
[46] C. E. Moore, *Atomic Energy Levels*, Natl. Bur. Stand. Ref. Data Ser., Natl. Bur. Stand. (U.S. GPO, Washington, D.C., 1971), Vol. 35.
[47] J. N. L. Connor, H. Sun, and J. M. Hutson, J. Chem. Soc. Faraday Trans. **86**, 1649 (1990).
[48] M. D. Pattengill, R. A. LaBudde, and R. B. Bernstein, J. Chem. Phys. **55**, 5517 (1971).
[49] A. Messiah, *Mécanique Quantique* (Dunod, Paris, 1965), Sec.III.